Radiology

ORIGINAL RESEARCH • GENITOURINARY IMAGING

Amide Proton Transfer-weighted MRI in Predicting Histologic Grade of Bladder Cancer

Huanjun J. Wang, MD, PhD • Qian Cai, MD* • Yiping P. Huang, MD • Meiqin Q. Li, MD • Zhihua H. Wen, MD • Yingyu Y. Lin, MD, PhD • Longyuan Y. Ouyang, MD • Long Qian, PhD • Yan Guo, MD, PhD*

From the Department of Radiology, The First Affiliated Hospital, Sun Yat-Sen University, 58 Zhongshan Road 2, Guangzhou 510080, PR China (H.J.W., Q.C., Y.H., M.L., Z.W., Y.L., L.O., Y.G.); and Department of MR Research, GE Healthcare, Beijing, PR China (L.Q.). Received July 20, 2021; revision requested September 13; revision received April 13, 2022; accepted May 12. **Address correspondence to** Y.G. (email: *gyan@mail.sysu.edu.cn*).

Supported by the National Natural Science Foundation of China (grant 82071989), Natural Science Foundation of Guangdong Province (grant 2021A1515012243), 2021 SKY Imaging Science and Research Fund of China International Medical Foundation (grant Z-2014-07-2101-12), and Kelin New Star Talent Program of The First Affiliated Hospital, Sun Yat-sen University (grant R08028).

* H.J.W. and Q.C. contributed equally to this work.

Conflicts of interest are listed at the end of this article.

See also the editorial by Milot in this issue.

Radiology 2022; 000:1–8 • https://doi.org/10.1148/radiol.211804 • Content codes: MR GU

Background: Bladder cancer is classified into high and low grades with different clinical treatments and prognoses. Thus, accurate preoperative evaluation of the histologic grade through imaging techniques is essential.

Purpose: To investigate the potential of amide proton transfer-weighted (APTw) MRI in evaluating the grade of bladder cancer and to evaluate whether APTw MRI can add value to diffusion-weighted imaging (DWI) at MRI.

Materials and Methods: In this single-center prospective study, participants with pathologic analysis–confirmed bladder cancer with no previous treatment, lesions larger than 10 mm, and adequate MRI quality were enrolled from July 2020 to September 2021 in a university teaching hospital. All participants underwent preoperative multiparametric MRI, including APTw MRI and DWI. The mean APTw and apparent diffusion coefficient (ADC) values of the primary tumor were measured independently by two radiologists. Receiver operating characteristic curves were generated to evaluate the diagnostic performance of these quantitative parameters.

Results: In total, 83 participants (mean age, 64 years ± 13 [SD]; 72 men) were evaluated: 51 with high-grade and 32 with low-grade bladder cancer. High-grade bladder cancer showed higher APTw values (6% [IQR, 4%–12%] vs 2% [IQR, 1%–3%]; $P < .001$) and lower ADC values (0.92×10^{-3} mm^2/sec ± 0.17 vs 1.21×10^{-3} mm^2/sec ± 0.25; $P < .001$) than low-grade bladder cancer. The area under the receiver operating characteristic curve (AUC) of APTw and ADC for differentiating low- and high-grade bladder cancer was similar (0.84 for both; $P = .94$). Moreover, the combination of the two techniques improved the diagnostic performance (AUC, 0.93; all $P = .01$).

Conclusion: The combination of amide proton transfer-weighted and diffusion-weighted MRI has the potential to improve the histologic characterization of bladder cancer by differentiating low- from high-grade cancers.

Online supplemental material is available for this article.

Bladder cancer is one of the most common malignant tumors of the urinary tract worldwide (1). Bladder cancer can be stratified into high- and low-grade cancers (2). The prognosis and treatment strategies differ between high- and low-grade cancers, especially for non–muscle-invasive bladder cancer (3,4). For patients with low-grade non–muscle-invasive bladder cancer, transurethral resection of bladder tumor is generally recommended, whereas those with high-grade non–muscle-invasive or muscle-invasive bladder cancer frequently require more intensive treatment such as radical cystectomy, systemic chemotherapy, and radiation therapy (5,6). Therefore, the accurate preoperative evaluation of the histologic grade of bladder cancer is of great clinical significance.

The reference standard procedure for the preoperative grading of bladder cancer is transurethral resection or cystoscopic biopsy (7). However, these procedures are invasive and carry the risk of undergrading the cancer (8). Undergrading can result in insufficient cure, such as incomplete resection, and further lead to tumor recurrence or metastasis. Diffusion-weighted imaging (DWI) at MRI and diffusion kurtosis MRI have been developed as noninvasive imaging markers for predicting the histologic grade of bladder cancer (8–14). However, it is a challenge to predict histologic grade accurately and noninvasively. Therefore, further development of other noninvasive quantitative methods for predicting tumor grade is desired.

Amide proton transfer-weighted (APTw) MRI, a subtype of chemical exchange saturation transfer imaging, is a molecular MRI technique that mainly measures the chemical transfer properties of amide protons located at a chemical shift of 3.5 ppm (15,16). The APTw value reflects the concentrations of mobile macromolecules, such as proteins and peptides. Previous studies have demonstrated that APTw MRI is useful for evaluating the

Abbreviations

ADC = apparent diffusion coefficient, APTw = amide proton transfer-weighted, AUC = area under the receiver operating characteristic curve, DWI = diffusion-weighted imaging, MTR_{asym} = magnetization transfer ratio asymmetry

Summary

Amide proton transfer-weighted MRI has potential in improving the diagnostic performance of diffusion-weighted MRI for high-grade bladder cancer.

Key Results

- In this prospective study of 83 participants with confirmed bladder cancer lesions larger than 10 mm who underwent preoperative MRI, high-grade cancers showed higher amide proton transfer-weighted (APTw) values than low-grade cancers (6% vs 2%; $P < .001$).
- The APTw and apparent diffusion coefficient (ADC) values had similar diagnostic performances (area under the receiver operating characteristic curve [AUC], 0.84 for both; $P = .94$), and the combination of APTw and ADC improved the diagnostic performance (AUC, 0.93; all $P = .01$).

histologic grade of tumors, such as brain gliomas, hepatocellular carcinoma, rectal cancer, and endometrioid endometrial adenocarcinoma (17–22). However, the finding of APTw MRI in evaluating the grade of bladder cancer has not previously been well established in the literature.

Therefore, this study aimed to investigate the potential of amide proton transfer-weighted (APTw) MRI in evaluating the histologic grade of bladder cancer and to evaluate whether APTw MRI can add diagnostic value to diffusion-weighted MRI of the bladder.

Materials and Methods

The institutional review board of the First Affiliated Hospital, Sun Yat-sen University (ie, the university teaching hospital) approved this single-center prospective study, and informed consent was obtained from all study participants. One author (L.Q.) is an employee of GE Healthcare (China; Beijing). Other authors (H.J.W., Q.C., Y.P.H., M.Q.L., Z.H.W., Y.Y.L., L.Y.O., Y.G), who are not employed by GE Healthcare, had control of the data and information submitted for publication.

Study Sample

From July 2020 to September 2021, participants suspected of having bladder tumors were initially enrolled and underwent pelvic MRI including APTw MRI and DWI. The inclusion criteria were as follows: no neoadjuvant treatment, including radiation therapy and chemotherapy, before MRI examination; pathologic analysis–confirmed urothelial carcinoma of the bladder; participants with nodular lesions with a maximum diameter larger than 10 mm or plaque-like lesions with a thickness larger than 10 mm; and adequate image quality for analysis.

Exclusion criteria were as follows: no surgery, benign lesions of the bladder and other subtypes of bladder cancer such as squamous or small cell carcinoma, neoadjuvant chemotherapy before MRI, nodular lesions smaller than 10 mm or plaque-like lesions with a thickness smaller than 10 mm, and inadequate image quality for analysis. Tumors with the largest volume were selected in participants with multifocal tumors. All tumors were resected and underwent pathologic examination separately. Histologic grade was determined according to the 2004 World Health Organization/International Society of Urological Pathology classification.

Subgroups of the study sample were reported in a prior study (14), which investigated the diagnostic performance of synthetic MRI for evaluating the grade of bladder cancer. APTw and synthetic MRI are two different advanced MRI techniques; therefore, these participants overlapping with the previous study were different and there was no conflict.

Image Acquisition

A 3.0-T MRI system (Signa Pioneer; GE Healthcare) with a 32-channel body coil was used for image acquisition. All study participants were required to urinate 2 hours before the MRI examination. No further drinking or urination was allowed until the end of MRI examination. APTw MRI and DWI were added to the routine scan sequences including T1-weighted, T2-weighted, and dynamic contrast-enhanced MRI. Axial APTw images were acquired on the basis of a three-dimensional fast spin-echo sequence. In the chemical exchange saturation transfer preparation module, a pseudocontinuous pulse was applied with a total duration of 2 seconds and a saturation power level of 2.0 μT. APTw images were then separately acquired at seven frequency offsets (±7, ±4, ±3.5, and ±3.0 ppm), and extra images (M0) were measured without saturation at 5000 Hz for reference. In addition, corresponding B_0 maps were measured by using a multiple gradient-echo sequence for B_0 inhomogeneity correction. The APTw image was computed as the magnetization transfer ratio asymmetry (MTR_{asym}) at 3.5 ppm, which was calculated on the basis of the following equation: MTR_{asym} = M (−3.5 ppm)/M0–M (3.5 ppm)/M0. The total scan time for APTw MRI was 10 minutes 54 seconds.

DWI (*b* values of 50 and 1000 sec/mm^2) were performed on axial and oblique sagittal planes perpendicular to the tumor base by using a single-shot echo planar sequence. Apparent diffusion coefficient (ADC) maps were generated from the DWI images on the scanner console. Dynamic contrast-enhanced MRI with one precontrast and plus five sets of contrast-enhanced images were acquired with a Liver Acquisition with Volume Acceleration–Flex sequence before and after intravenous injection of 0.2 mL/kg of gadoteric acid (gadoteric acid meglumine salt injection; Jiangsu Hengrui Medicine) at a rate of 2 mL/sec. The detailed scan parameters are presented in Table E1 (online). The total MRI acquisition time was about 40 minutes.

Image Analysis

The Vesical Imaging Reporting and Data System score was assigned for each participant by a radiologist (H.J.W., with 11 years of experience in pelvic MRI). The quality of APTw and ADC images were independently evaluated by two radiologists (H.J.W. and Q.C., with 11 and 4 years of experience in pelvic MRI, respectively) without knowledge of the pathologic information. The APTw image quality was assessed by using a five-point Likert scale (Table E2 [online]) referring to relevant

literature (23,24). ADC image quality was evaluated by using a quantitative four-point scale (Table E3 [online]) as described in the literature (25). Discordance between the two radiologists was resolved by consensus.

All quantitative parameters were obtained by using software (ITK-SNAP software, version 2.2.0; *http://www.itksnap.org*). Two radiologists (Q.C. and Y.P.H., with 4 and 2 years of experience in pelvic MRI, respectively) performed the measurements and were blinded to the pathologic results. Regions of interest (ROIs) were manually delineated on DWI scans (b = 50 sec/mm^2) and B_0 maps in participants with minimum image quality score of 3. ROIs were placed along the periphery of the tumor at the level of the largest area of the mass and on the section above and below this level. Artifacts, blood vessels, regions of necrosis, and tumor stalk were avoided. Then, ROIs were copied to the APTw and ADC maps. Figure E1 (online) shows an example of ROI delineation. The mean APTw and ADC values were automatically calculated for the ROIs. All analytic results from the two radiologists were reviewed by a senior radiologist (H.J.W., with 11 years of experience in pelvic MRI). When ambiguous cases were considered by the senior radiologist, consensus was obtained after discussion. The mean values of APTw and ADC measured by the two radiologists were used for the final analysis.

Statistical Analysis

Statistical analyses were performed by using software (SPSS software version 25.0, IBM; MedCalc statistical software version 12.7, *https://www.medcalc.org*; and R version 4.1.0, R Foundation for Statistical Computing).

A sample size of at least 26 participants was required based on the following: power, 80%; two-sided significance level indicated by a P value of .05; alternative hypothesis of the area under the receiver operating characteristic curve (AUC), 0.80, compared with the null hypothesis of the AUC, 0.50; and an allocation ratio of sample sizes in the negative and positive groups of 1.

The interobserver agreements for ROI measurements were calculated by using the intraclass correlation coefficients. For image quality assessment, the interobserver agreement was evaluated by κ analysis.

The differences in the mean APTw and ADC values between low- and high-grade bladder cancer were assessed by using the independent sample t test or Mann-Whitney U test. The paired Wilcoxon signed-rank test was applied to evaluate the differences in image quality between APTw or ADC images and T2-weighted images.

Receiver operating characteristic curve analysis was performed to evaluate the diagnostic performance outcomes of these quantitative parameters for discriminating low-grade from high-grade bladder cancer. Optimal cut points for APTw and ADC values were derived by using the Youden index. In addition, the diagnostic performance of the combined parameters was determined based on predicted probability calculated by using binary logistic regression analysis. The DeLong test was used for the comparison of receiver operating characteristic curves (26). Differences with P value less than .05 were considered to indicate statistical significance.

Results

Participant Characteristics

The study enrolled 180 participants. Ninety-seven participants were excluded from the analysis due to no surgery (n = 34), benign lesions of the bladder (n = 21), other subtypes of bladder cancer such as squamous or small cell carcinoma (n = 3), neoadjuvant chemotherapy before MRI (n = 2), bladder lesions smaller than 10 mm (n = 28), and inadequate image quality for analysis (n = 9). Figure 1 shows the flowchart of the participant selection process.

The study ultimately included 83 participants with bladder cancer, including 72 men (87%) and 11 women (13%), and the mean age was 64 years ± 13 (SD). All participants underwent surgery (11 participants underwent radical cystectomy, two participants underwent partial cystectomy, and 70 participants underwent transurethral resection of bladder tumor) within 2 weeks (range, 1–19 days) after undergoing MRI. Six participants with recurrent bladder tumors and the remaining 79 participants referred to the hospital for the first time were not administered any treatment before undergoing MRI. Twenty-three of 51 (45%) had muscle invasion, and 11 (22%) had lymphatic metastasis among the participants with high-grade bladder cancer. And among 32 participants with low-grade bladder cancer, only one (3%) had muscle invasion and none had lymphatic metastasis. The clinical and pathologic features of these participants are shown in Table 1.

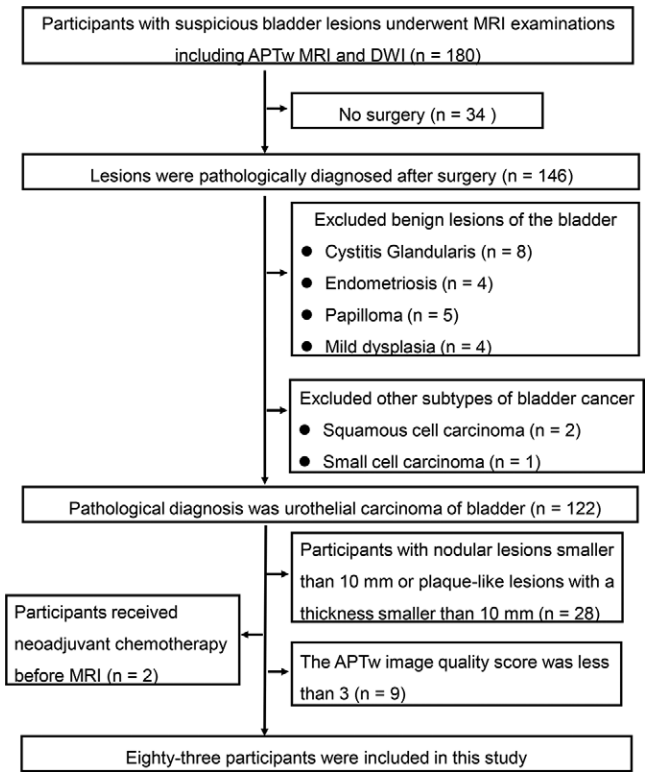

Figure 1: Flowchart shows the participant selection process. APTw = amide proton transfer-weighted, DWI = diffusion-weighted MRI.

Image Quality Assessment

Among 122 study participants with pathologic confirmation, two underwent neoadjuvant chemotherapy before undergoing MRI and 28 had bladder lesions that were smaller than 10 mm. The remaining participants (n = 92) underwent APTw and ADC evaluation of image quality. Two independent readers rated the image quality of APTw MRI significantly lower than that of T2-weighted MRI (median score, 4 vs 5; $P < .001$). There was no evidence of a difference in the image quality scores between ADC images and T2-weighted MRI (median score, 4; $P = .08$). Figure 2 shows the image quality scores for APTw and ADC images. The interreader agreements between the two readers for the APTw (κ, 0.86; $P < .001$) and ADC (κ, 0.66; $P < .001$) image quality scores were excellent and good, respectively. Figures E2 and E3 (online) show four participants with APTw image quality scores of 2–5 (Fig E2 [online]) and two participants with ADC image quality scores of 3 and 4 (Fig E3 [online]).

Interobserver Agreement of the Quantitative Measurements

The intraclass correlation coefficients of the APTw and ADC values measured by the two radiologists were 0.98 (95% CI: 0.97, 0.99) and 0.98 (95% CI: 0.97, 0.98), respectively.

Table 1: Clinical Characteristics of Study Participants with Bladder Cancer

Variable	Total (n = 83)	Histologic Bladder Cancer Grade		P Value
		High Grade (n = 51)	Low Grade (n = 32)	
Age (y)*	64 ± 13	64 ± 12	64 ± 13	.95
Sex				.87
Male	72	44 (61)	28 (39)	
Female	11	7 (64)	4 (36)	
VI-RADS				<.001
2†	56	26 (46)	30 (54)	
3‡	6	5 (83)	1 (17)	
4§	2	2 (100)	0	
5‖	19	18 (95)	1 (5)	
Lesion location				.78
Side wall	77	47 (61)	30 (39)	
Trigone	6	4 (67)	1 (33)	
Diameter of lesion				.82
≥3 cm	35	22 (63)	13 (37)	
<3 cm	48	29 (60)	19 (40)	
No. of lesions				.81
Single	61	37 (61)	24 (39)	
Multiple	22	14 (64)	8 (36)	

Note.—Unless otherwise indicated, data are numbers of participants; data in parentheses are percentages. BCa = bladder cancer, VI-RADS = Vesical Imaging Reporting and Data System.

* Data are means ± SD.

† Nonmuscle-invasive bladder cancer, 52 participants; muscle-invasive bladder cancer, four participants.

‡ Nonmuscle-invasive bladder cancer, four participants; muscle-invasive bladder cancer, two participants.

§ Muscle-invasive bladder cancer.

‖ Nonmuscle-invasive bladder cancer, three participants; muscle-invasive bladder cancer, 16 participants.

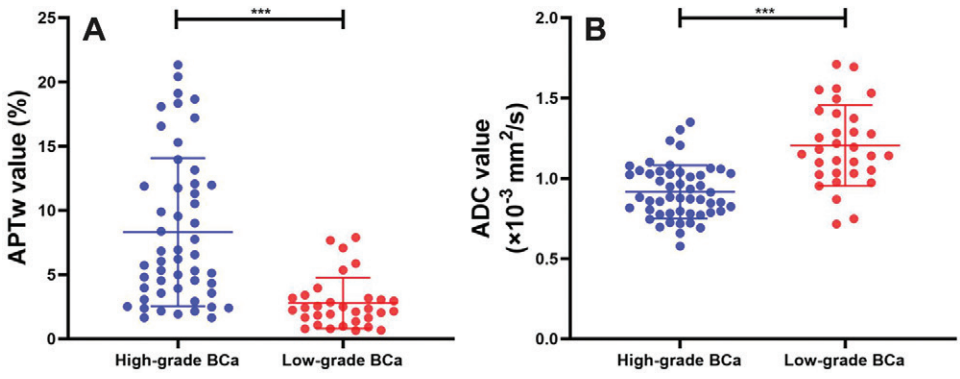

Figure 2: Scatter plots of the **(A)** amide proton transfer-weighted (APTw) and **(B)** apparent diffusion coefficient (ADC) values between high-and low-grade bladder cancer. *** $P < .001$. BCa = bladder cancer.

Comparisons of the APTw and ADC Values between Low- and High-Grade Cancer

The APTw and ADC values for evaluating the histologic grade are summarized in Table 2 and Figure 3. High-grade cancer had higher APTw values than low-grade cancer (6% [IQR, 4%–12%] vs 2% [IQR, 1%–3%]; $P < .001$). The ADC values of high-grade cancer were lower than those of low-grade cancer (0.92×10^{-3} mm²/sec ± 0.17 vs 1.21×10^{-3} mm²/sec ± 0.25; $P < .001$). Figures 4 and 5 show MRI scans in two participants with low- and high-grade cancer, respectively.

Diagnostic Performance Outcomes of the APTw and ADC Values in Evaluating Histologic Grade

The receiver operating characteristic analysis results are shown in Table 3 and Figure 6. The AUC of the APTw value for distinguishing low- and high-grade bladder cancer was 0.84 (95% CI: 0.76, 0.92) and the optimal cutoff value was 4% (sensitivity, 78% [40 of 51; 95% CI: 64, 88]; specificity, 81% [26 of 32; 95% CI: 63, 92]).

For the ADC value, the AUC was 0.84 (95% CI: 0.74, 0.93) and the optimal cutoff value was 1.09 $\times 10^{-3}$ mm²/sec (sensitivity, 90% [46 of 51; 95% CI: 78, 96]; specificity, 69% [22 of 32; 95% CI: 50, 83]). There was no evidence of a difference between APTw and ADC values for differentiating low- from high-grade cancer (AUC, 0.84 for both; P = .94).

Moreover, combining the APTw and ADC values yielded a sensitivity of 78% (40 of 51; 95% CI: 64, 88), a specificity of 94% (30 of 32; 95% CI: 78, 99), and an AUC of 0.93 (95% CI: 0.87, 0.98). The combination of APTw and ADC values showed higher diagnostic performance compared with the single APTw or ADC value (APTw with ADC vs APTw or ADC, $P = .01$).

Discussion

Accurate preoperative evaluation of the histologic grade by bladder cancer is important because high- and low-grade cancers have different clinical treatments and prognoses. Our study evaluated the diagnostic potential of amide proton transfer-weighted (APTw) MRI and diffusion-weighted imaging (DWI) at MRI for differentiating high- and low-grade bladder cancer. Our results showed that high-grade cancers exhibited higher APTw values than low-grade cancers (6% [IQR, 4%–12%] vs 2% [IQR, 1%–3%]; $P < .001$). APTw and apparent diffusion coefficient (ADC) values for differentiating low- from high-grade cancers had similar diagnostic performance (area under the receiver operating characteristic curve [AUC], 0.84 for both; $P = .94$). In addition, the combination of APTw MRI and DWI had improved diagnostic performance (AUC, 0.93) compared with individual analysis of either technique (APTw with ADC vs APTw or ADC, $P = .01$). However, the image quality of APTw MRI was inferior to that of T2-weighted MRI (median score, 4 vs 5; $P < .001$).

Table 2: Comparisons of the Amide Proton Transfer-weighted and Apparent Diffusion Coefficient Values in High- and Low-grade Bladder Cancer

Parameter	High-grade Bladder Cancer	Low-grade Bladder Cancer	*P* Value
APTw (%)	6 (4–12)	2 (1–3)	<.001
ADC ($\times 10^{-3}$ mm^2/sec)	0.92 ± 0.17	1.21 ± 0.25	<.001

Note.—Normally distributed data are expressed as mean ± SD; other data are expressed as the median with first quartile and third quartile in parentheses. APTw = amide proton transfer weighted, ADC = apparent diffusion coefficient.

Our results showed that the APTw value of high-grade cancer was higher than that of low-grade cancer, which is consistent with the findings of previous studies on other tumors (17–22). Takayama et al (20) investigated the use of APTw MRI in estimating the histologic grade of endometrioid endometrial adenocarcinoma, indicating a positive correlation of the APTw value with the histologic grade in endometrioid endometrial adenocarcinoma. Moreover, a recent study (22) also reported that APTw MRI can be used to differentiate high- and low-grade gliomas in pediatric patients. These similar findings may be attributed to the higher mobile protein and peptide concentrations in high-grade tumors because high-grade tumors are characterized by rapid cell proliferation, increased protein expression, and high cellular density (27). Moreover, nuclear atypia, which was reported to induce the interaction of macromolecules with hydrophobic cell membranes and promote the release of proteins and peptides, might be another factor for the higher APTw value in high-grade tumors (28).

In addition, high-grade bladder cancer had lower ADC values, which is consistent with findings in previous studies (8–12,14). The ADC value, a diffusion coefficient reflecting the degree of diffusion of water molecules in tissues, is highly sensitive to cellularity changes. The higher density of tissue cells in high-grade tumors greatly restricts water molecule diffusion, which accounts for the lower ADC values in high-grade tumors.

Although APTw MRI is a promising noninvasive method for evaluating tumors at the molecular level, the image quality of APTw MRI was unsatisfactory compared with T2-weighted images. In most participants, the tumor boundary was poorly seen or even undetectable in APTw MRI without reference to the T2-weighted image. Law et al (24) also demonstrated that the image quality of APTw MRI was inferior to that of the anatomic image when applied to head and neck tumors. In addition, the spatial

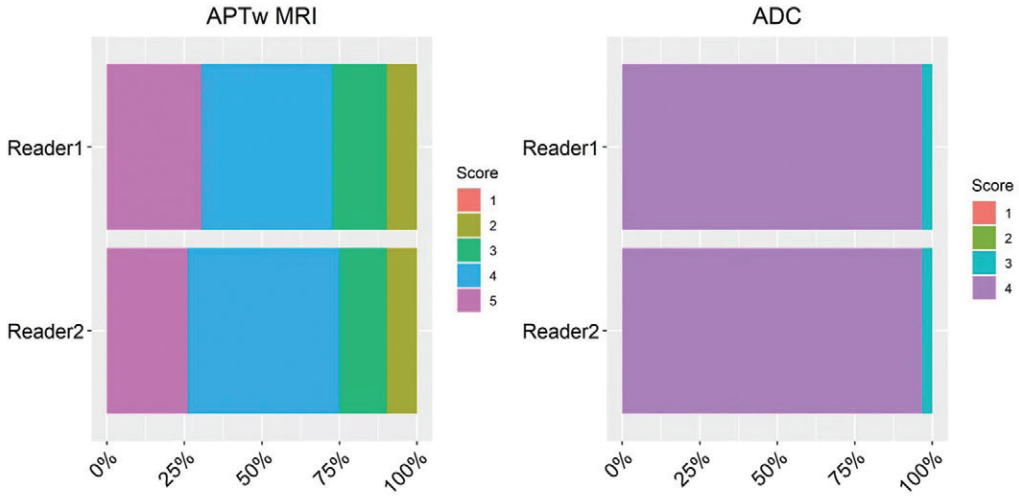

Figure 3: The image quality scores of the two readers for amide proton transfer-weighted (APTw) MRI and apparent diffusion coefficient (ADC) images.

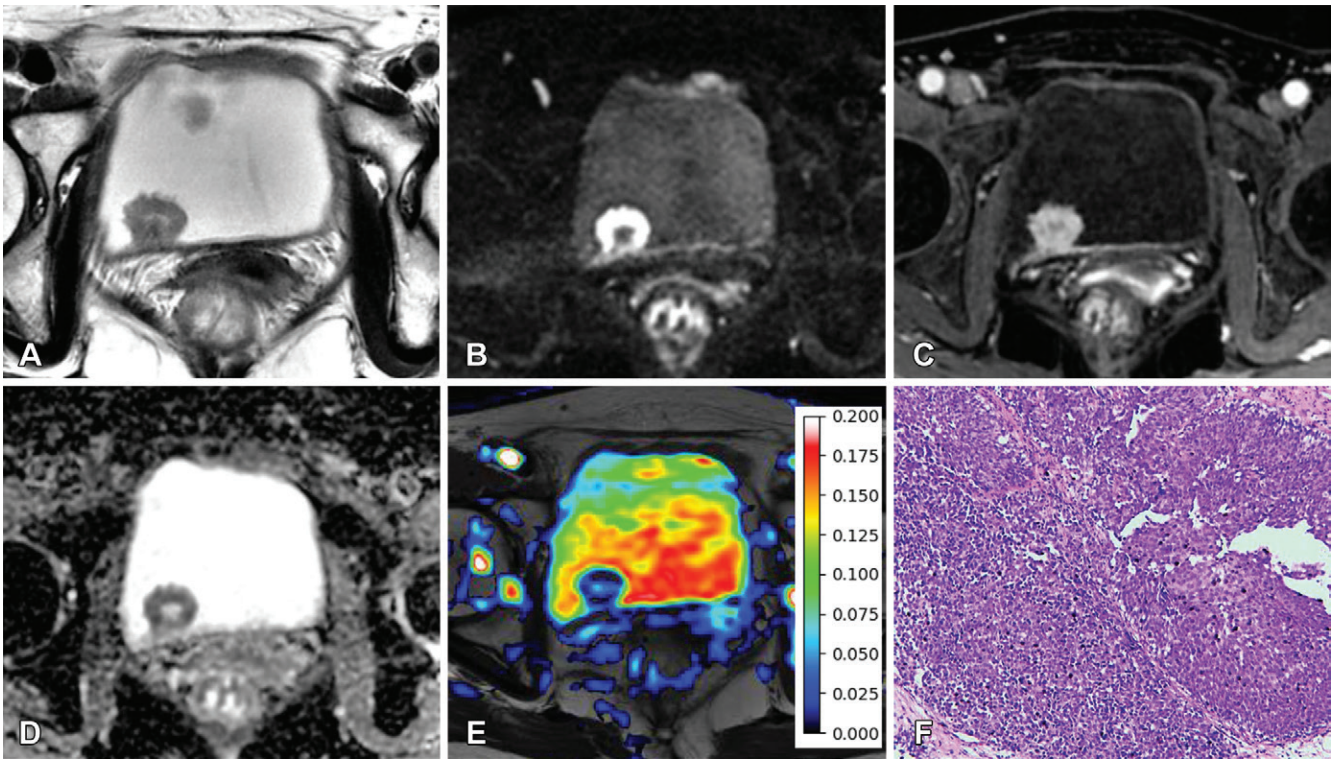

Figure 4: MRI scans in a 63-year-old woman with bladder cancer and a 20-mm tumor. Axial **(A)** T2-weighted image, **(B)** diffusion-weighted image (b = 1000 sec/mm^2), **(C)** dynamic contrast-enhanced image, **(D)** apparent diffusion coefficient (ADC) image, **(E)** amide proton transfer-weighted (APTw) image fused with T2-weighted image, and **(F)** microscopic image of hematoxylin-eosin staining (original magnification, ×100). **(E)** The color bar indicates the APTw value. The lesion is assigned a Vesical Imaging Reporting and Data System score of 2. The mean ADC and APTw values measured by the two radiologists are 1.11 × 10^{-3} mm^2/sec and 2%, respectively. Pathologic examination after transurethral resection showed no detrusor muscle invasion, and the histologic grade of the lesion was low grade.

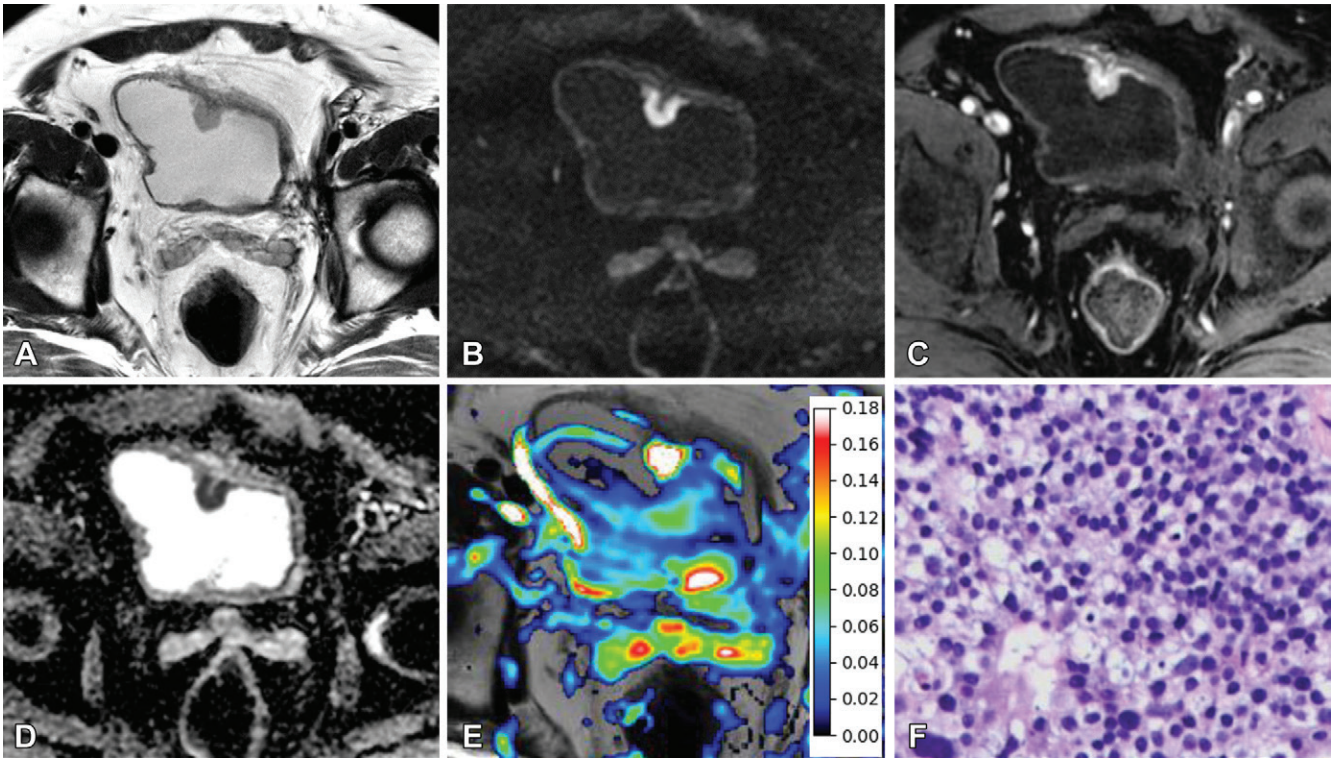

Figure 5: MRI scans in a 72-year-old man with bladder cancer and a 14-mm tumor. Axial **(A)** T2-weighted image, **(B)** diffusion-weighted image (b = 1000 s/mm^2), **(C)** dynamic contrast-enhanced image, **(D)** apparent diffusion coefficient (ADC) image, **(E)** amide proton transfer-weighted (APTw) image fused with T2-weighted image, and **(F)** microscopic image of hematoxylin-eosin staining (original magnification, × 100). The color bar indicates the APTw value. The lesion was assigned a Vesical Imaging Reporting and Data System score of 2. The mean ADC and APTw values measured by the two radiologists were 0.82 × 10^{-3} mm^2/sec and 17%, respectively. Pathologic examination after transurethral resection showed no detrusor muscle invasion, and the histologic grade of the lesion was high grade.

Table 3: Diagnostic Performance of the Amide Proton Transfer-weighted and Apparent Diffusion Coefficient Values in Differentiating Low- and High-grade Bladder Cancer

Parameter	AUC	*P* Value	Cutoff Value*	Sensitivity	Specificity
APTw	0.84 (0.76, 0.92)	.94	4	40/51 (64, 88)	26/32 (63, 92)
ADC	0.84 (0.74, 0.93)		1.09	46/51 (78, 96)	22/32 (50, 83)
APTw and ADC	0.93 (0.87, 0.98)		…	40/51 (64, 88)	30/32 (78, 99)

Note.—Unless otherwise indicated, data are the numerator/denominator and data in parentheses are 95% CIs. APTw = amide proton transfer weighted, ADC = apparent diffusion coefficient, AUC = area under the receiver operating characteristic curve.

* The cutoff value was determined using Youden index.

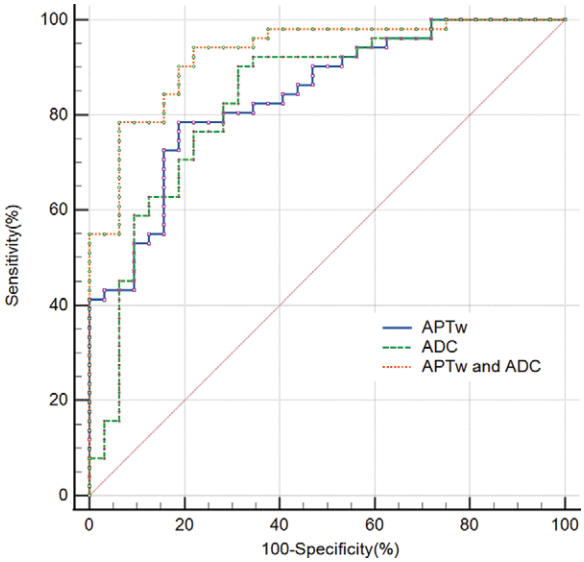

Figure 6: Receiver operating characteristic curves for differentiating low- and high-grade bladder cancer. The area under the receiver operating characteristic curves (AUC) of amide proton transfer-weighted (APTw) values, apparent diffusion coefficient (ADC) values, and the combination of the two were 0.84 (95% CI: 0.76, 0.92), 0.84 (95% CI: 0.74, 0.93), and 0.93 (95% CI: 0.87, 0.98), respectively. *P* values for comparison of the AUC for APTw, ADC values, and the combination of the two were .94 (APTw vs ADC) and .01 (APTw and ADC vs APTw or ADC).

resolution of APTw MRI was 1.6 × 2.1 × 8 mm^3, making it difficult to assess small bladder lesions. Twenty-eight participants with lesions smaller than 10 mm were excluded from the study because of the low spatial resolution of APTw MRI. In our study, the MTR_{asym} analysis defined as MTR_{asym} = M (−3.5 ppm)/M0 – M (3.5 ppm)/M0 was applied to quantify chemical exchange saturation transfer effect, which might include not only the pure amide proton transfer effect but may also relay the nuclear Overhauser effect, the conventional magnetization transfer effect, and the direct saturation effect (29). Therefore, the resultant chemical exchange saturation transfer effect quantified by MTR_{asym} analysis can only quantify the APTw but not the pure amide proton transfer signal (29).

There were several limitations in our study. First, the number of participants in our study sample was relatively small, and this was a single-center study. Second, ROI delineation was only performed at the level of the largest area of the lesion and on the slice above and below this level (not the whole lesion), which may have introduced some bias. Third, lesions smaller than 10 mm in size were excluded considering low spatial resolution of APTw MRI, which also might lead to a biased sample. Fourth, the acquisition time of chemical exchange saturation transfer–based three-dimensional APTw MRI was long, which may bring discomfort to some participants, especially older participants.

In conclusion, our study demonstrated that amide proton transfer-weighted (APTw) MRI is beneficial for evaluating the histologic grade of bladder cancer and provides additional information to improve the results of diffusion-weighted MRI. Further prospective studies containing larger sample sizes from multiple centers are needed to validate the stability and reproducibility of these results. Furthermore, some technical issues and challenges must be addressed in the follow-up studies, such as advanced APTw MRI and postprocessing methods to improve the image quality and well separate the pure amide proton transfer signal from contributions of other components, such as nuclear Overhauser-mediated chemical exchange saturation transfer effect.

Author contributions: Guarantors of integrity of entire study, **H.J.W., Q.C., Y.P.H., M.Q.L., Z.H.W., L.Q., Y.G.**; study concepts/study design or data acquisition or data analysis/interpretation, all authors; manuscript drafting or manuscript revision for important intellectual content, all authors; approval of final version of submitted manuscript, all authors; agrees to ensure any questions related to the work are appropriately resolved, all authors; literature research, all authors; clinical studies, **H.J.W., Q.C., Y.P.H., M.Q.L., Z.H.W., L.Y.O., L.Q., Y.G.**; statistical analysis, **Q.C., Y.P.H., M.Q.L., Z.H.W., Y.Y.L., L.Y.O., L.Q., Y.G.**; and manuscript editing, **H.J.W., Q.C., M.Q.L., Z.H.W., Y.Y.L., L.Q., Y.G.**

Disclosures of conflicts of interest: **H.J.W.** No relevant relationships. **Q.C.** No relevant relationships. **Y.P.H.** No relevant relationships. **M.Q.L.** No relevant relationships. **Z.H.W.** No relevant relationships. **Y.Y.L.** No relevant relationships. **L.Y.O.** No relevant relationships. **L.Q.** No relevant relationships. **Y.G.** No relevant relationships.

References

1. Siegel RL, Miller KD, Jemal A. Cancer statistics, 2018. CA Cancer J Clin 2018; 68(1):7–30.
2. Wang G, McKenney JK. Urinary Bladder Pathology: World Health Organization Classification and American Joint Committee on Cancer Staging Update. Arch Pathol Lab Med 2019;143(5):571–577.
3. Babjuk M, Burger M, Zigeuner R, et al. EAU guidelines on non-muscle-invasive urothelial carcinoma of the bladder: update 2013. Eur Urol 2013;64(4):639–653.
4. Pan CC, Chang YH, Chen KK, Yu HJ, Sun CH, Ho DM. Prognostic significance of the 2004 WHO/ISUP classification for prediction of recurrence, progression, and cancer-specific mortality of non-muscle-invasive urothelial tumors of the urinary bladder: a clinicopathologic study of 1,515 cases. Am J Clin Pathol 2010;133(5):788–795.
5. Alfred Witjes J, Lebret T, Compérat EM, et al. Updated 2016 EAU Guidelines on Muscle-invasive and Metastatic Bladder Cancer. Eur Urol 2017;71(3):462–475.

6. Flaig TW, Spiess PE, Agarwal N, et al. Bladder Cancer, Version 3.2020, NCCN Clinical Practice Guidelines in Oncology. J Natl Compr Canc Netw 2020;18(3):329–354.
7. Bellmunt J, Orsola A, Leow JJ, et al. Bladder cancer: ESMO Practice Guidelines for diagnosis, treatment and follow-up. Ann Oncol 2014;25(Suppl 3):iii40–iii48.
8. Wang HJ, Pui MH, Guo Y, et al. Multiparametric 3-T MRI for differentiating low-versus high-grade and category T1 versus T2 bladder urothelial carcinoma. AJR Am J Roentgenol 2015;204(2):330–334.
9. Takeuchi M, Sasaki S, Ito M, et al. Urinary bladder cancer: diffusion-weighted MR imaging--accuracy for diagnosing T stage and estimating histologic grade. Radiology 2009;251(1):112–121.
10. Kobayashi S, Koga F, Yoshida S, et al. Diagnostic performance of diffusion-weighted magnetic resonance imaging in bladder cancer: potential utility of apparent diffusion coefficient values as a biomarker to predict clinical aggressiveness. Eur Radiol 2011;21(10):2178–2186.
11. Kobayashi S, Koga F, Kajino K, et al. Apparent diffusion coefficient value reflects invasive and proliferative potential of bladder cancer. J Magn Reson Imaging 2014;39(1):172–178.
12. Sevcenco S, Ponhold L, Heinz-Peer G, et al. Prospective evaluation of diffusion-weighted MRI of the bladder as a biomarker for prediction of bladder cancer aggressiveness. Urol Oncol 2014;32(8):1166–1171.
13. Wang F, Chen HG, Zhang RY, et al. Diffusion kurtosis imaging to assess correlations with clinicopathologic factors for bladder cancer: a comparison between the multi-b value method and the tensor method. Eur Radiol 2019;29(8):4447–4455.
14. Cai Q, Wen Z, Huang Y, et al. Investigation of Synthetic Magnetic Resonance Imaging Applied in the Evaluation of the Tumor Grade of Bladder Cancer. J Magn Reson Imaging 2021;54(6):1989–1997.
15. Zhou J, Lal B, Wilson DA, Laterra J, van Zijl PC. Amide proton transfer (APT) contrast for imaging of brain tumors. Magn Reson Med 2003;50(6):1120–1126.
16. Zhou J, Blakeley JO, Hua J, et al. Practical data acquisition method for human brain tumor amide proton transfer (APT) imaging. Magn Reson Med 2008;60(4):842–849.
17. Togao O, Yoshiura T, Keupp J, et al. Amide proton transfer imaging of adult diffuse gliomas: correlation with histopathological grades. Neuro Oncol 2014;16(3):441–448.
18. Choi YS, Ahn SS, Lee SK, et al. Amide proton transfer imaging to discriminate between low- and high-grade gliomas: added value to apparent diffusion coefficient and relative cerebral blood volume. Eur Radiol 2017;27(8):3181–3189.
19. Nishie A, Takayama Y, Asayama Y, et al. Amide proton transfer imaging can predict tumor grade in rectal cancer. Magn Reson Imaging 2018;51:96–103.
20. Takayama Y, Nishie A, Togao O, et al. Amide Proton Transfer MR Imaging of Endometrioid Endometrial Adenocarcinoma: Association with Histologic Grade. Radiology 2018;286(3):909–917.
21. Wu B, Jia F, Li X, Li L, Wang K, Han D. Comparative Study of Amide Proton Transfer Imaging and Intravoxel Incoherent Motion Imaging for Predicting Histologic Grade of Hepatocellular Carcinoma. Front Oncol 2020;10:562049.
22. Zhang H, Yong X, Ma X, et al. Differentiation of low- and high-grade pediatric gliomas with amide proton transfer imaging: added value beyond quantitative relaxation times. Eur Radiol 2021;31(12):9110–9119.
23. He YL, Li Y, Lin CY, et al. Three-dimensional turbo-spin-echo amide proton transfer-weighted mri for cervical cancer: A preliminary study. J Magn Reson Imaging 2019;50(4):1318–1325.
24. Law BKH, King AD, Ai QY, et al. Head and Neck Tumors: Amide Proton Transfer MRI. Radiology 2018;288(3):782–790.
25. Chen H, Chen L, Liu F, Lu J, Xu C, Wang L. Diffusion-weighted magnetic resonance imaging in bladder cancer: comparison of readout-segmented and single-shot EPI techniques. Cancer Imaging 2019;19(1):59.
26. DeLong ER, DeLong DM, Clarke-Pearson DL. Comparing the areas under two or more correlated receiver operating characteristic curves: a nonparametric approach. Biometrics 1988;44(3):837–845.
27. Chen W, Li L, Yan Z, et al. Three-dimension amide proton transfer MRI of rectal adenocarcinoma: correlation with pathologic prognostic factors and comparison with diffusion kurtosis imaging. Eur Radiol 2021;31(5):3286–3296.
28. Meng N, Wang X, Sun J, et al. Application of the amide proton transfer-weighted imaging and diffusion kurtosis imaging in the study of cervical cancer. Eur Radiol 2020;30(10):5758–5767.
29. Dou W, Lin CE, Ding H, et al. Chemical exchange saturation transfer magnetic resonance imaging and its main and potential applications in pre-clinical and clinical studies. Quant Imaging Med Surg 2019;9(10):1747–1766.